Magnetic and magnetoelectric dynamics in RMn_2O_5 (R = Gd and Eu)

2004 J. Phys.: Condens. Matter 16 4325

(http://iopscience.iop.org/0953-8984/16/24/014)

INSTITUTE OF PHYSICS PUBLISHING JOURNAL OF PHYSICS: CONDENSED MATTER

J. Phys.: Condens. Matter **16** (2004) 4325–4334 PII: S0953-8984(04)77480-9

Magnetic and magnetoelectric dynamics in RMn_2O_5 (R = Gd and Eu)

E Golovenchits and V Sanina

Ioffe Physical-Technical Institute of the Russian Academy of Sciences, 194021, Saint Petersburg, Russia

E-mail: e.golovenchits@mail.ioffe.ru

Received 1 March 2004
Published 4 June 2004
Online at stacks.iop.org/JPhysCM/16/4325
doi:10.1088/0953-8984/16/24/014

Abstract

The dynamics of ferroelectromagnetic (multiferroic) crystals RMn_2O_5 (R = Eu and Gd), showing magnetic and ferroelectric phase transitions with close transition temperatures (40 and 30 K for R = Eu and Gd, respectively), was studied in the frequency and temperature ranges 20–300 GHz and 5–50 K, respectively. It was found that magnetic resonance spectra of $GdMn_2O_5$ are characteristic for the homogeneous long-range magnetic order both of the antiferomagnetic Mn-subsystem and Gd magnetic subsystem, possessing a large ferromagnetic moment. In other RMn_2O_5 crystals (with nonmagnetic or weakly magnetic rare-earth ions) incommensurate or space-modulated magnetic structures in Mn-subsystem are present. The strong Gd–Mn and Gd–Mn–Gd exchange interactions are responsible for the homogeneous magnetic state. A strong effect of the magnetic state on the ferroelectric state was discovered in $GdMn_2O_5$ crystal. The temperature of the ferroelectric phase transition in $GdMn_2O_5$ is shifted to the lower temperature as compared with other RMn_2O_5 crystals. Mixed magnetoelectric excitations in $GdMn_2O_5$ were observed for the first time.

1. Introduction

The family of ferroelectromagnetic crystals RMn_2O_5—$R^{3+}Mn^{3+}Mn^{4+}O_5^{2-}$—(R: rare-earth ions from Pr to Lu, Y, and Bi) shows magnetic and ferroelectric long-range order at temperatures lower than 30–40 K. In traditional ferroelectromagnetics, such as boracities, hexagonal manganites and orthorhombic perovskite-type crystals $BiFeO_3$, the Curie temperature of ferroelectric phase transition usually considerably exceeds the temperature of the magnetic phase transition, i.e. the interactions responsible for the ferroelectricity considerably exceed exchange interactions responsible for the magnetic order. In the family of manganite crystals, RMn_2O_5, investigated in this paper, magnetic and ferroelectric orders arise at close

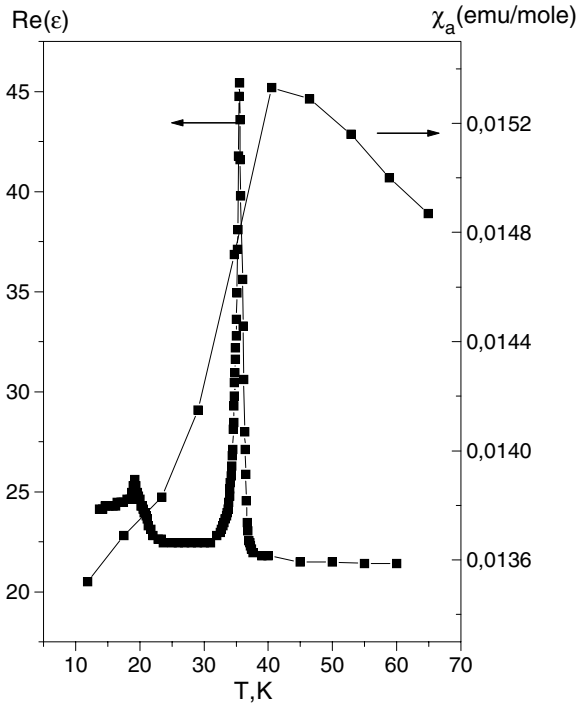

Figure 1. Temperature dependences of the ac dielectric and magnetic susceptibilities for $EuMn_2O_5$ [1, 2].

temperatures. Figure 1 demonstrates a coincidence of the magnetic and ferroelectric phase transition temperatures in $EuMn_2O_5$ [1, 2].

It is possible that in RMn_2O_5 crystals both magnetic and ferroelectric orders are associated with the same Jahn–Teller Mn^{3+} ions. Thus structural distortions and magnetic state are interrelated. If the spin–orbital interaction is dominant in Jahn–Teller interactions, the temperatures of magnetic and structural transitions can coincide [3, 4]. In this case it is natural to expect a strong relationship between magnetic and ferroelectric states. In the $GdMn_2O_5$ crystals investigated a considerable effect of magnetic state on the ferroelectricity has indeed been observed.

At room temperature RMn_2O_5 crystals are characterized by an orthorhombic crystal structure—space group *Pbam* [5]. The structure of these crystals is demonstrated in figure 2.

In RMn_2O_5 crystals there are two low-temperature phase transitions with simultaneous changes in the magnetic and structural states— T_1 (15–20 K) and T_2 (35–40 K). The nature of the first transition is not clear in detail now, the second one is a simultaneous magnetic and ferroelectric phase transition ($T_2 = T_{N,C}$) [1, 2, 6–8]. The low-temperature structural state is investigated in detail only in $EuMn_2O_5$ [9]. The symmetry of this crystal is described by the space groups $P2_1am$ and $P1a1$ at temperatures 40–22 K and $T < 22$ K, respectively.

The incommensurate magnetic structure with the propagation vector $\mathbf{k} = (\mathbf{1/2}, \mathbf{0}, \mathbf{z})$ and $T_N \simeq 35$–40 K, where the z-value depends on the type of R-ion ($z = 0.3$–0.38), is realized usually in the Mn-subsystem of RMn_2O_5 crystals. There is antiferromagnetic structure along the a-axis and incommensurate (or space-modulated) structure along the c-axis.

Magnetic, dielectric and magnetoelectric (ME) properties of several crystals with different R ions were studied in [1, 2, 6–8, 10, 11]; the neutron diffraction data can be found in [9, 12].

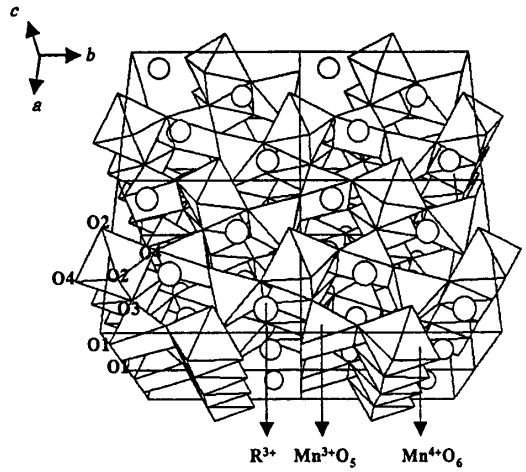

Figure 2. Crystal structure of RMn_2O_5 ($2a \times 2b \times 2c$).

This paper presents the first study of the microwave dynamics in RMn_2O_5 with the Eu^{3+} ion, which is nonmagnetic in the ground state ($^7F_0$), and the Gd^{3+} ion, whose spin moment in the ground state ($^8S_{7/2}$) is the greatest among the R-ions. Note that a bulk static magnetization study of $EuMn_2O_5$ crystals [2] shows that the quantum-mechanical admixture of the excited magnetic state ($^7F_1$) to the ground state of Eu^{3+} ions is a negligible quantity. Dynamics of crystals with R = Gd is found to be substantially different from that with R = Eu due to the effect of a strong magnetic R-subsystem on magnetic and magnetoelectric properties. The preliminary data of $GdMn_2O_5$ dynamics study were published in our paper [13]. We also present the results of magnetic and dielectric studies of $GdMn_2O_5$, allowing us to complete the data [8].

$EuMn_2O_5$ forms an incommensurate magnetic structure with simultaneously existing ferroelectric order with ordering temperatures $T \simeq 36$ K [1, 2, 6]. Antiferromagnetic ordering in $GdMn_2O_5$ arises in the Mn-subsystem at the temperature close to the magnetic ordering temperature for $EuMn_2O_5$, but near 30 K an additional phase transition occurs [8]. As follows from the presented results, the low-temperature ($T \leqslant 30$ K) $GdMn_2O_5$ phase is characterized by the homogeneous antiferromagnetic state in the Mn-subsystem and the magnetic state with the large ferromagnetic moment in the Gd-subsystem. In addition, the ferroelectric Curie temperature is close to the temperature of the homogeneous magnetic state formation ($T_C \simeq 30$ K).

2. Experimental results

The dynamic studies were performed with a quasi-optical spectrometer using the transmission scheme. The source of microwave radiation was backward-wave tubes, and the receiver was a detector based on the InSb crystal cooled with liquid helium. The single crystals were grown by the method of spontaneous crystallization described in [1]. Crystals have the forms of well-faceted parallelepipeds with typical dimensions 5 mm × 4 mm × 4 mm. Plates ∼0.5 mm thick were cut normally to the crystal a, b and c axes. The plates by their cutting planes (the planes of the samples) were oriented normally to the direction of electromagnetic wave propagation. Microwave electric and magnetic field vectors (**e** and **h**, respectively) were in the plane of the sample. An external permanent magnetic field (H_0) of up to 2.0 T was also applied in the plane of the sample.

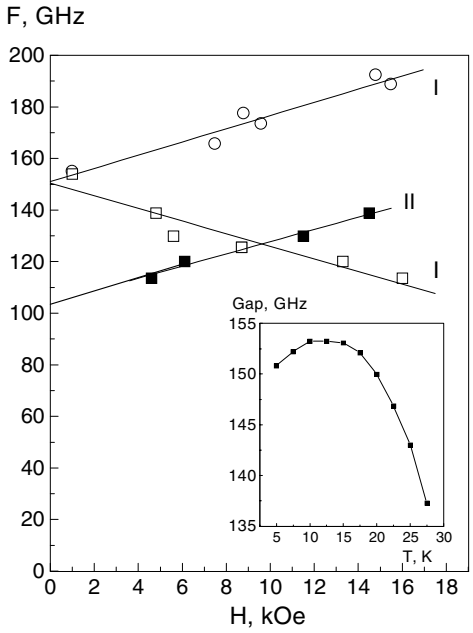

Figure 3. Frequency dependences of magnetic resonances on external magnetic field, oriented along the a-axis, of the $GdMn_2O_5$ plate with the ab plane (sample 2 according to the classification of figure 5); $H_0 \parallel a$, $T = 5$ K. In the inset the temperature dependence of the gap in spectrum I is shown.

The magnetic field dependences of the relative absorption coefficient

$$\Gamma_{F,T} = 1 - P(H)/P(H_{max}) \tag{1}$$

were studied at fixed frequencies and temperatures. Here $P(H)$ and $P(H_{max})$ are the microwave power transmitted through the sample at the current field value and at the field value corresponding to maximum transmission, respectively. In addition, we studied the temperature dependences of the relative absorption coefficients

$$\Gamma_F = 1 - P(T)/P(T_{max}) \tag{2}$$

in the absence of magnetic field at fixed frequencies. $\Gamma_{F,T}(H)$ and $\Gamma_F(T)$ dependences were used to construct the frequency and field dependences of the absorption coefficient at fixed temperatures (magnetic resonance spectra).

The magnetic resonance absorption spectra over the operating frequency range (20–300 GHz) on scanning of the magnetic field were observed only in $GdMn_2O_5$ and for $H_0 \parallel a$ orientation only (see figure 3). Two characteristic magnetic resonance spectra with linearly depended resonance frequencies on the field were found. The gap values (the resonance frequencies at $H_0 = 0$) are 150 (I) and 100 GHz (II), respectively. One could see in the inset in figure 3, that the gap in spectrum I changes with temperature as the order parameter with a critical temperature of $T \sim 35$–40 K and decreases to 130 GHz as temperature increases to $T \sim 30$ K. The gap of the spectrum II is practically independent of the temperature up to 30 K. The intensity temperature dependences of the signals I and II were different also (see figure 4). The intensity of signal I changed with temperature as the order parameter with a critical temperature of $T \sim 35$–40 K (as the gap). In contrast to the gap, the absorption

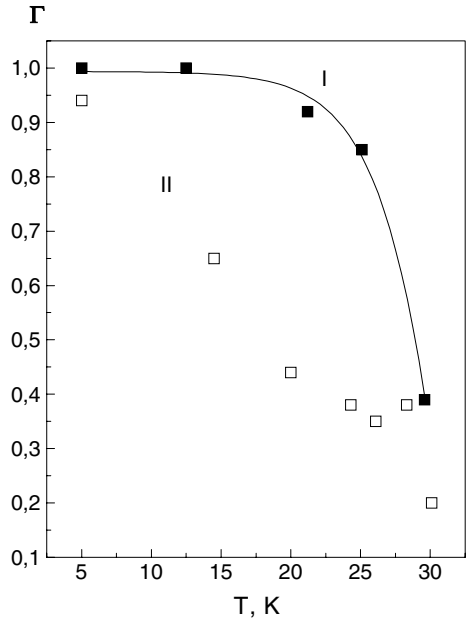

Figure 4. Temperature dependences of the intensity of signal I (frequency $F = 165.7$ GHz) and signal II ($F = 113.6$ GHz) along the a-axis.

coefficient for signal II decreased much more sharply near 15–20 K, but kept a noticeable value up to 30 K.

Absorption lines were also observed in the absence of a magnetic field (see figure 5). Unlike the magnetic resonances, whose intensities decreased as the temperature approached 30 K, the intensity of these lines had maxima at $T \simeq 30$ K. The shape of $\Gamma_F(T)$-dependences were determined by the orientation of the microwave electric field **e** with respect to the crystal axes a, b and c. The lines of this type were excited mainly by the microwave electric field **e** and likely were determined by the dynamics of the lattice near the phase transition at $T \simeq 30$ K. A temperature hysteresis was observed for the absorption lines. As it can be seen from the inset in figure 5, the peaks of Γ_F near 30 K depend on the frequency and attain their maximum near 130 GHz. It is worth remembering that this frequency is close to the gap value for the magnetic resonances (signal I) near 30 K. The external magnetic field also modified the lines of an electric nature (see figure 6). The influence was most pronounced for the $H_0 \parallel a$ orientation. The absorption maximum then shifted to the frequency corresponding to that of signal I at the given magnetic field value.

In $EuMn_2O_5$ only low-intensity absorption signals were observed over the full operating frequency range of 30–300 GHz at temperatures near 36–40 K. These signals seem to be caused by the anomalies of the dynamic susceptibilities near the phase transition to incommensurate magnetic and ferroelectric states.

A magnetic and dielectric susceptibility study has been performed for $GdMn_2O_5$ which allowed us to add the data [8] (see figure 7). The real part of the dielectric susceptibility (real ϵ) shows a very sharp and intensive maximum near $T \simeq 30$ K similar to that observed for $EuMn_2O_5$ at $T = 36$ K [1, 2, 6] near the antiferromagnetic and ferroelectric phase transition (see figure 1). This anomaly, together with the data on magnetoelectric susceptibility and pyrocurrent [8] leads us to the conclusion that the dielectric susceptibility anomaly

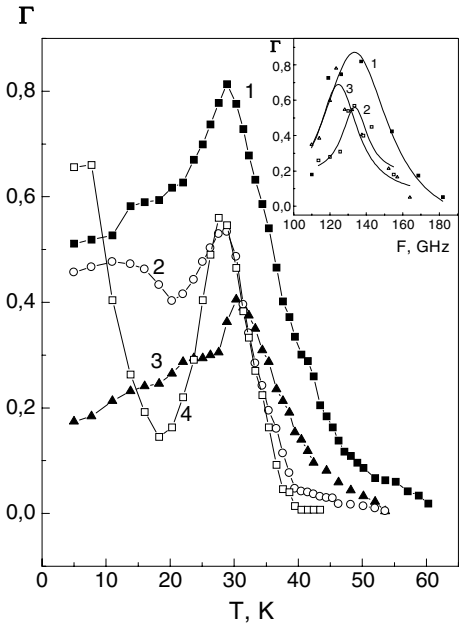

Figure 5. Temperature dependences of the relative absorption coefficient Γ at $H_0 = 0$ for $GdMn_2O_5$ samples: (1) the ab plane, $\mathbf{e} \parallel a$, frequency $F = 137$ GHz; (2) the ac plane, $\mathbf{e} \parallel a$, frequency $F = 129.9$ GHz; (3) the ab plane, $\mathbf{e} \parallel b$, frequency $F = 135.1$ GHz; (4) the ab plane, $\mathbf{e} \parallel a$, frequency $F = 137$ GHz; (5) the bc plane, $\mathbf{e} \parallel c$, frequency $F = 132.1$ GHz. Shown in the inset are the frequency dependencies of Γ at the maximum of the absorption line near the $T \simeq 30$ K for samples 1, 2 and 3.

characterizes the transition to the ferroelectric state with polarization oriented along the b-axis. The maximum of the real ϵ at $T \simeq 30$ K in $GdMn_2O_5$ was observed when **e** was oriented along all crystal principal axes. But the jump value was two orders of magnitude larger at $\mathbf{e} \parallel b$.

The magnetic susceptibility of $GdMn_2O_5$ measured by the induction method is shown in the inset of figure 7. The temperature and magnetic field dependences of the susceptibility are characteristic for the magnetic order state with the large ferromagnetic moment oriented along the **a**-axis. The susceptibility is saturated in a weak external magnetic field and decreases with increasing temperature starting with $T \sim 30$ K. But the tail of susceptibility extends to the higher temperatures.

3. Analysis of magnetic and ME dynamics

We associate the absorption lines in $GdMn_2O_5$, which are observed in the absence of magnetic field and have maxima near $T \simeq 30$ K, with the magnetoelectric's excitation dynamics. Basic experimental arguments for such an interpretation are the following: the mainly electrical nature of these absorption signals; the closeness of the magnetic resonance frequencies to the frequencies of the absorption lines of the electrical nature; the influence of the external magnetic field on these lines. We observed the ME dynamics both near the phase transition ($T \simeq 30$ K) and at low temperatures (in the temperature interval of electrical-type lines and magnetic resonance's overlap) (see figure 5). The theoretical aspects of ME-excitation dynamics are considered in [14].

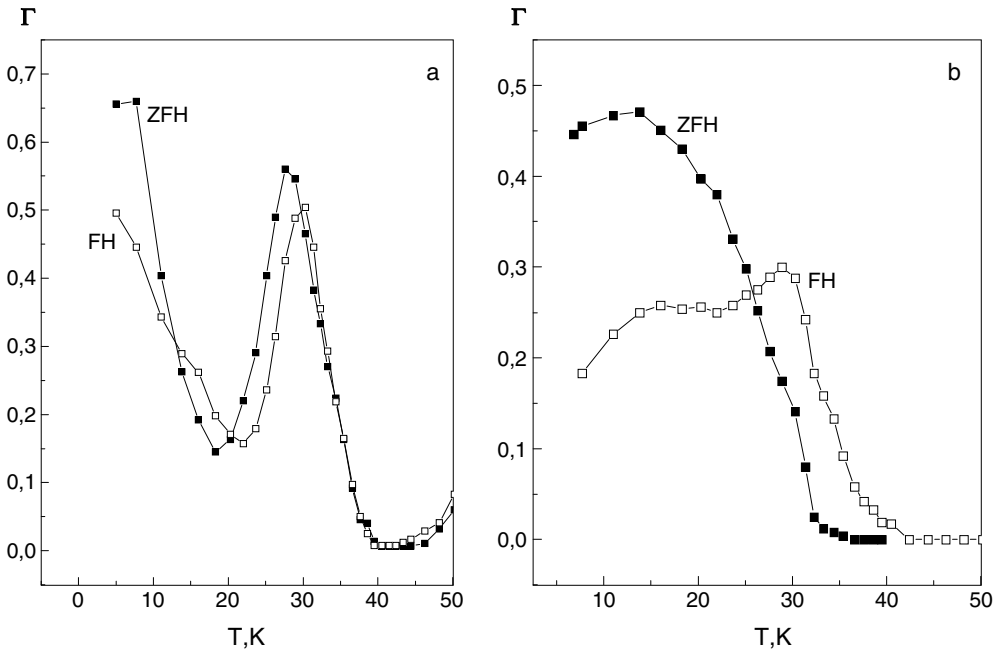

Figure 6. The same dependences as in figure 5 for samples 4 (a) and 1 (b) taken at $H_0 = 0$ under the conditions of slow heating (ZFH) after preliminary slow cooling to $T = 5$ K and under slow heating in a nonzero magnetic field $H_0 \neq 0$ (FH). The magnetic field was applied at $T = 5$ K. For sample 4: $H_0 = 1.6$ T, $H_0 \parallel c$, frequency $F = 132.1$ GHz; for sample 1: $H_0 = 1.86$ T, $H_0 \parallel a$, frequency $F = 168.5$ GHz.

As noted above, in ferroelectromagnetics the temperature of the ferroelectric phase transition usually considerably exceeds that of the magnetic ordering. In such a case the ferroelectric modes with frequencies comparable with the magnetic excitation frequencies can exist only near the ferroelectric transition temperatures (soft ferroelectric modes). But magnetic ordering at such high temperatures disappears. In $GdMn_2O_5$ the temperatures of magnetic and ferroelectric transitions are closely matched to each other. This fact has allowed us to observe for the first time mixed ME dynamics.

Let us consider the magnetic dynamic properties. The character of spectrum I in figure 3 is very specific and is characteristic for the antiferromagnetic resonance of homogeneous (with the propagation vector $\mathbf{k} = (\mathbf{1/2}, \mathbf{0}, \mathbf{0})$) antiferromagnets, without weak ferromagnetic moment, with light axes anisotropy, in the case of magnetic field orientation along the anisotropy axes (in our case, along the a-axis). In this case the magnetic field dependences of antiferromagnetic resonance frequencies have the form

$$\omega_{1,2} = \sqrt{2H_E H_A} \pm \gamma H_0, \tag{3}$$

where H_E and H_A are the exchange and anisotropy fields, respectively, and γ is the gyromagnetic ratio. For homogeneous antiferromagnets the temperature dependences of the gap and intensity of resonance signals coincide with the temperature dependence of the magnetic order parameter. Such a type of temperature dependence of the gap and intensity for the spectrum I is indeed observed (see the inset in figures 3 and 4). Thus, the magnetic resonance data (spectrum I) witness that in $GdMn_2O_5$ the homogeneous uniaxial antiferromagnetic state without weak ferromagnetic moment exists. This state we assign to the Mn subsystem, since

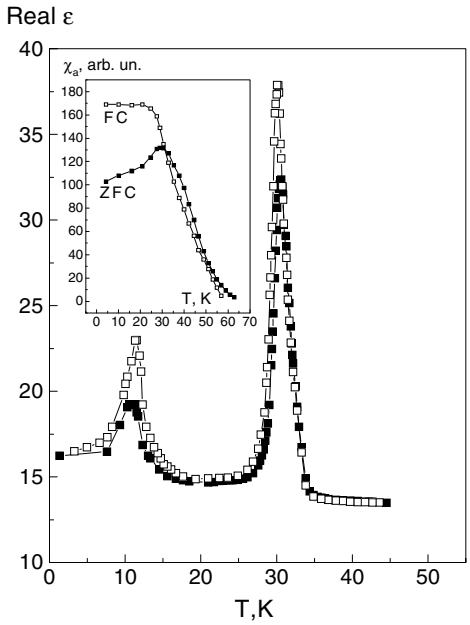

Figure 7. Temperature dependences of the real part of dielectric susceptibility for $GdMn_2O_5$ at frequency 10 kHz in the $\mathbf{e} \parallel b$ orientation. The solid and open symbols correspond to heating and cooling of the sample, respectively. Shown in the inset are the temperature dependences of magnetic susceptibility (in arbitrary units) for $GdMn_2O_5$; frequency 10 kHz, $\mathbf{h} \parallel a, h = 4$ Oe. The curves were recorded for the sample cooling in the absence of an external magnetic field (ZFC) and in $H_0 = 40$ Oe, $H_0 \parallel a$ (FC), respectively.

the transition temperature of the antiferromagnetic order parameter for spectrum I is 36–40 K. For spectrum I the value $\gamma = 2.75 \pm 0.15$ and corresponds to a g factor close to the spin value $g = 2$. From the gap value at $T = 5$ K one could estimate the internal effective fields for the Mn subsystem: exchange field $H_E \simeq 400$ kOe; the anisotropy field $H_A \simeq 4$ kOe; the spin-flop field $H_{SF} = \sqrt{2H_E H_A} \simeq 55$ kOe.

The dependence $\omega(H_0)$ for spectrum II has the form

$$\omega = \Delta\omega + \gamma H_0. \tag{4}$$

Spectrum II is characteristic for the ferromagnetic resonance with the gap. Taking into account the temperature dependences of the gap and intensity for spectrum II, we relate this spectrum with the magnetic ordered Gd-subsystem possessing the ferromagnetic moment. The magnetic susceptibility data (see the inset in figure 7) also show the existence of the ferromagnetic moment in $GdMn_2O_5$ crystal. The slope of $\omega(H_0)$ dependency is the same as that of spectrum I, i.e. it corresponds to the spin value $g = 2$. This agrees with the ground state of Gd ions. The ferromagnetic resonance gap of the Gd subsystem $\Delta\omega$ is mainly determined by the internal effective magnetization field operating on the Gd subsystem from the side of antiferromagnetic ordered the Mn subsystem (induced by Gd–Mn exchange interaction). The value of this field is about 40 kOe.

Thus the magnetic dynamics data, along with the static magnetization data, give one a possibility to definitely attribute a magnetic structure of the each magnetic subsystems in $GdMn_2O_5$ crystal. By contrast the magnetic susceptibility and magnetization data give the information about the integral magnetic state of crystal.

Note that in [11] antiferromagnetic structures for both magnetic subsystems (Mn and Gd) in $GdMn_2O_5$, with different Neel temperatures—35 and 15 K, respectively, were assumed for the discussion of magnetic behaviour in a strong magnetic field. A jump of the magnetization along the a-axis at the magnetic field $H_0 \simeq 60$ kOe was observed in [11], which was considered by the authors as the spin-flop transition in the Gd subsystem. Experimental results in [11] do not contradict our results if we suppose that the Gd-subsystem is a ferromagnetic ordered one and Mn-subsystem is an antiferromagnetic ordered without weak ferromagnetic moment. The jump of the magnetization we attribute to the spin-flop transition in the antiferromagnetic Mn-subsystem. Our estimation of the spin-flop field value from the magnetic dynamics data agrees with the jump field value in [11].

Let us discuss now the reason for the appearance of the homogeneous magnetic state in $GdMn_2O_5$. Recall that in RMn_2O_5 crystals with nonmagnetic or weak magnetic R-ions (particularly in $EuMn_2O_5$) the incommensurate or space-modulated magnetic structure in the Mn subsystem is usually realized. However, the appearance of the homogeneous magnetic state in the Mn subsystem of $EuMn_2O_5$ was observed earlier [10] in a strong magnetic field (near 20 T). We suppose that the homogeneous antiferromagnetic state in the Mn subsystem in $GdMn_2O_5$ is caused by the strong uniform effective magnetic field acting from the ferromagnetic ordered Gd subsystem. The magnetic ordering state with large ferromagnetic moment can arise in the Gd subsystem due to the polarization exchange interaction Gd–Mn–Gd [15]. The corresponding exchange interaction is written as

$$\mathcal{H} = \sum_{ij} B_{ij}^{\mathrm{Gd-Gd}} S_i^{\mathrm{Gd}} S_j^{\mathrm{Gd}}, \qquad B_{ij}^{\mathrm{Gd-Gd}} = A_{ik}^{\mathrm{Gd-Mn}} \chi_{kl}^{\mathrm{Mn}} A_{lj}^{\mathrm{Mn-Gd}}. \tag{5}$$

Here $B_{ij}^{\mathrm{Gd-Gd}}$ is the tensor of polarization Gd–Mn–Gd exchange interaction via spin excitations or spin fluctuations in Mn-subsystem; $A_{ik}^{\mathrm{Gd-Mn}}$ is the tensor of Gd–Mn exchange interaction; χ_{kl}^{Mn} is the magnetic susceptibility of Mn-subsystem [15]. Note that the magnetic long-range order in the Gd subsystem, induced by the polarization exchange interaction, can be of antiferromagnetic or ferromagnetic type, consistent with the symmetry of the crystal. By contrast the magnetic structure of Gd-subsystem, induced by the intrinsic magnetization field originating from Gd–Mn exchange interaction, has to be the same symmetry as the magnetic structure of the Mn subsystem [15]. Thus, the magnetic state with large ferromagnetic moment along the a-axis in the Gd subsystem is most likely caused by the polarization exchange interaction (Gd–Mn–Gd).

The nonzero mean spin value Gd subsystem $\langle S_i^{\mathrm{Gd}} \rangle$ arises due to the Gd–Mn–Gd interaction. As a result, the intrinsic molecular exchange field

$$H_j^{\mathrm{Mn}} = A_{ij}^{\mathrm{Mn-Gd}} \langle S_i^{\mathrm{Gd}} \rangle, \tag{6}$$

acting on the Mn subsystem from the ordered Gd subsystem, arises. This field is an analogue of the strong external magnetic field, which induced in $EuMn_2O_5$ a phase transition from the space-modulated to homogeneous antiferromagnetic state. In turn the magnetization field, acting on the Gd subsystem from the ordered Mn subsystem,

$$H_i^{\mathrm{Gd}} = A_{ij}^{\mathrm{Mn-Gd}} \langle S_j^{\mathrm{Mn}} \rangle, \tag{7}$$

extends the magnetic order of the Gd subsystem up to 30 K.

It should be noted that there are additional experimental data indicating the existence in $GdMn_2O_5$ of the homogeneous magnetic state. Indeed, in this crystal a linear ME effect of very high value was observed [8]. As shown in [16] the linear ME effect is possible only for crystals with a homogeneous magnetic structure with ferromagnetic moment. For spatially modulated structure the linear ME effect is cancelled, and only the ME effect of higher order can exist.

As noted above, in $GdMn_2O_5$ the temperature of the ferroelectric phase transition is notably lower than the Curie temperature for $EuMn_2O_5$ (30 K instead of 36 K, correspondingly). In addition, the temperature of ferroelectric transition in $GdMn_2O_5$ coincides with the temperature of homogeneous magnetic state arising (but not with the temperature of antiferromagnetic incommensurate state formation as in $EuMn_2O_5$). This fact demonstrates the effect of the homogeneous magnetic state on the ferroelectricity. Such magnetic ordering seems to partly depress the ferroelectricity.

Thus the presence of magnetic Gd ions and the existence of the strong Gd–Mn exchange interaction substantially influence the magnetic, magnetoelectric and ferroelectric properties of $GdMn_2O_5$ crystals. In fact, the homogeneous magnetic order states arise in Mn- and Gd-subsystems, the high value linear ME effect is observed at $T \leqslant 30$ K and the ferroelectric order temperature T_C shifts to lower value in comparison with $EuMn_2O_5$. Comparable values of the magnetic and ferroelectric interactions lead to the strong interrelation between magnetic and ferroelectric states in $GdMn_2O_5$ and allow us to observe the mixed ME dynamics.

Acknowledgments

This research was supported by RFBR (grant 02-02-16140a), and part by the grants of the Presidium of the Russian Academy of Sciences ('Quantum Macrophysics') and of the Division of Physical Sciences of the Russian Academy of Sciences.

References

[1] Sanina V A, Sapozhnikova L M, Golovenchits E I and Morozov N V 1988 *Sov. Phys.—Solid State* **30** 1736
[2] Golovenchits E I, Morozov N V, Sanina V A and Sapozhnikova L M 1992 *Sov. Phys.—Solid State* **34** 56
[3] Kugel K and Khomsky D 1982 *Sov. Phys.—Usp.* **25** 231
[4] Babinskii A V, Ginzburg S L, Golovenchits E I and Sanina V A 1993 *JETP Lett.* **53** 299
[5] Abrahams S C and Burnshtein J L 1967 *Phys. Rev.* B **46** 3776
[6] Doi T and Kohn K 1992 *Phase Transit.* **38** 273
[7] Inomata A and Kohn K 1996 *J. Phys.: Condens. Matter* **8** 2673
[8] Tsujino H and Kohn K 1992 *Solid State Commun.* **83** 639
[9] Polyakov V, Plakhty V and Bonnet M 2001 *Physica* B **297** 208
[10] Popov Yu F, Kadomtseva A M and Vorob'ev G P 1998 *J. Magn. Magn. Mater.* **188** 237
[11] Popov Yu F, Kadomtseva A M and Vorob'ev G P 2003 *Phys. Solid State* **45** 2155
[12] Wilkinson C, Sinclair F and Gardner P 1981 *J. Phys. C: Solid State Phys.* **14** 1671
[13] Golovenchits E I and Sanina V A 2003 *JETP Lett.* **78** 88
[14] Smolenskii G A and Chupis I E 1982 *Sov. Phys.—Usp.* **25** 475
[15] Golovenchits E I and Sanina V A 1984 *Sov. Phys.—Solid State* **26** 996
[16] Popov Yu F, Kadomtseva A M and Vorob'ev G P 1994 *Ferroelectrics* **162** 135